J. Ziebs, J. Meersmann,* H. J. Kühn,* N. Hülsmann* and J. Olschewski**

Multiaxial Thermomechanical Behaviour of IN 738 LC Alloy

REFERENCE Ziebs, J., Meersmann, J., Kühn, H. J., Hülsmann, N. and Olschewski, J., **Multiaxial thermomechanical behaviour of IN 738 LC alloy**, *Multiaxial Fatigue and Design*, ESIS 21 (Edited by A. Pineau, G. Cailletaud, and T. C. Lindley) 1996, Mechanical Engineering Publications, London, pp. 83–96.

ABSTRACT A study was undertaken to develop an understanding of the fatigue life on IN 738 LC under simple, and simulated in-service operating thermomechanical cycling (TMF) in air. The experiments were conducted in the temperature ranges 450–950°C, 450–760°C and 600–850°C. Results indicate that the lives differ with strain–temperature phasing. Diamond cycles gave the longest lives. Simple nonproportional strain paths with a 90° phase angle gave the shortest lives. Life prediction models can be derived by simple thermomechanical low-cycle fatigue tests. Significant parameters governing cycles to failure were found to be the mechanical inelastic strain range, the maximum stress range, the total strain range and the energy criteria $\Delta\varepsilon_{min}\Delta\sigma_{max}$ and $\Delta\varepsilon_{tot}\Delta\sigma_{max}$. TMF life can be approximated by isothermal life at maximum and minimum temperature since the saturated response of IN 738 LC is the same for both tests methods. However, the TMF response cannot be predicted completely using only isothermal parameters. The J_2-theory can also be used to describe the TMF behaviour at highest and lowest temperature.

1 Introduction

High-temperature components such as turbine blades experience, during service, triaxial thermomechanical stress–strain fields. Predictions of blade behaviour or life using only isothermal behaviour or simple thermomechanical tests based on sequences of linear ramps may not be appropriate for many conditions due to complex microstructural dependence on deformation and temperature history. Generally, inelastic behaviour of a metal is due to its past history of deformation and temperature. Under repeated strain–temperature cycles a material may harden/soften or remain the same, depending on the initial state. Non-symmetric stress cycles in the plastic range may cause progressive strain ratchetting; and non-symmetric strain cycles in the plastic range will cause a progressive mean stress relaxation.

In low cycle TMF fatigue the sequencing of loading and temperature variations can influence the fatigue life. Both shearing and normal strains/stresses under multiaxial loading are important in distinguishing the type of fracture.

The majority of TMF tests have been carried out using simple thermal mechanical cycles; linear and diamond sequences (**1, 2**), Fig. 1. Accurate life

*Federal Institute for Materials Research and Testing, Unter den Eichen 87, D-12205, Berlin.

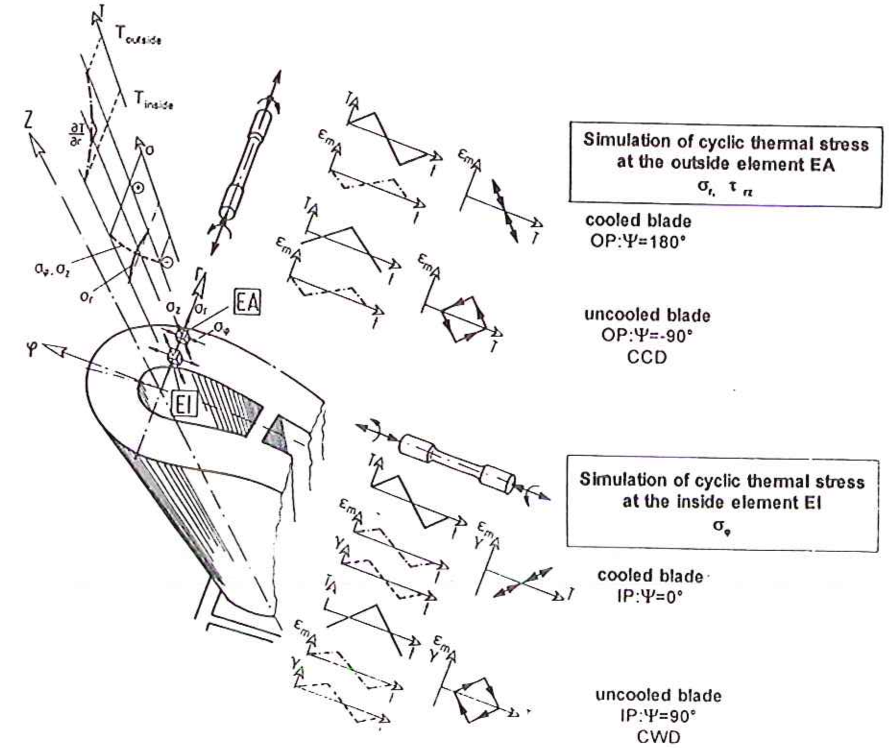

Fig 1 Simulation of cyclic thermal stresses in a blade with simple thermomechanical cycles (linear and diamond)

T	temperature	CWD	clockwise dir.
t	time	γ	shear strain
Ψ	phase	ε_m	mech. strain
IP	in-phase	$\tau_{f\varphi}$	shear stress
OP	out-of-phase	σ_φ	tang. thermal stress
CCD	counter-clockwise dir.	σ_r	radial thermal stress

assessment, however, requires properties of the blade material to be tested under actual service conditions. The complex thermal and mechanical history during a typical cycle of operation, consisting of start-up, steady-state operation and shut-down is shown in Fig. 2 for a first-stage blade. As shown in this figure, the maximum tensile strain occurs during shut-down of the machine at low temperature. During steady-state operation, the surface of the leading edge of the blade is in tangential compressive strain $\varepsilon_{m\varphi}$ due to tangential thermal stress σ_φ from the internal air cooling. The compressive strains $\varepsilon_{m\varphi}$ at the surface relax during service due to surface bulk temperature difference, and thereby increase the maximum tensile strain during shut-down.

To understand the differences between simple and complex TMF cycles and to improve life prediction capabilities, biaxial tension–torsion thermomechanical

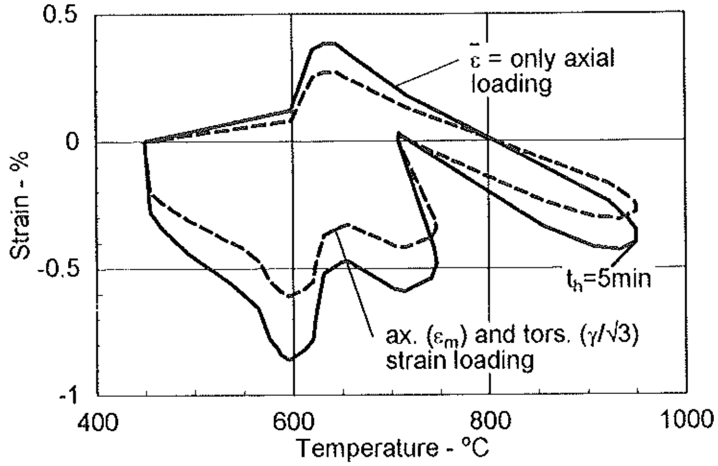

Fig 2 Start-up and shut-down axial and shear strain–temperature profile of a blade leading edge.

testing of actual blade cycles, with and without hold times, has been carried out. This paper will focus primarily on the development of a multiaxial life prediction method based on observed phenomena. The thermomechanical response of IN 738 LC is also investigated using the classical plasticity theory.

2 Material and Experimental Procedure

2.1 *Material*

The material studied was the cast Ni-base alloy IN 738 LC typically used for turbine blades. The chemical composition of IN 738 LC in weight percent is 0.105 C; 15.9997 Cr; 8.7 Co; 1.77 Mo; 1.9 Ta; 3.45 Ti; 3.4 Al; 2.71 W; 0.09 Si; 0.03 Mn; 0.82 Nb; 0.3 Fe; 0.037 Zn and balance Ni. The material was solution treated at 1120°C for two hours, air cooled and then aged at 850°C for 24 h. The microstructure consisted mostly of cuboidal γ' in a γ-matrix. The volume fraction of γ' was approximately 43 percent.

Thin-walled tubular specimens, 200 mm in total length, 50 mm gauge length, 26.5 mm outside diameter and 1.5 mm thickness in the gauge section were used. The specimens were supplied as cast-to-size tubes, Fig. 3.

2.2 *Experimental set-up*

The thermomechanical tests were conducted on an MTS tension–torsion-internal pressure closed-loop servohydraulic test machine under computer control. This system is equipped with an induction heating unit and a temperature monitoring device. The specimens can be subjected to controlled

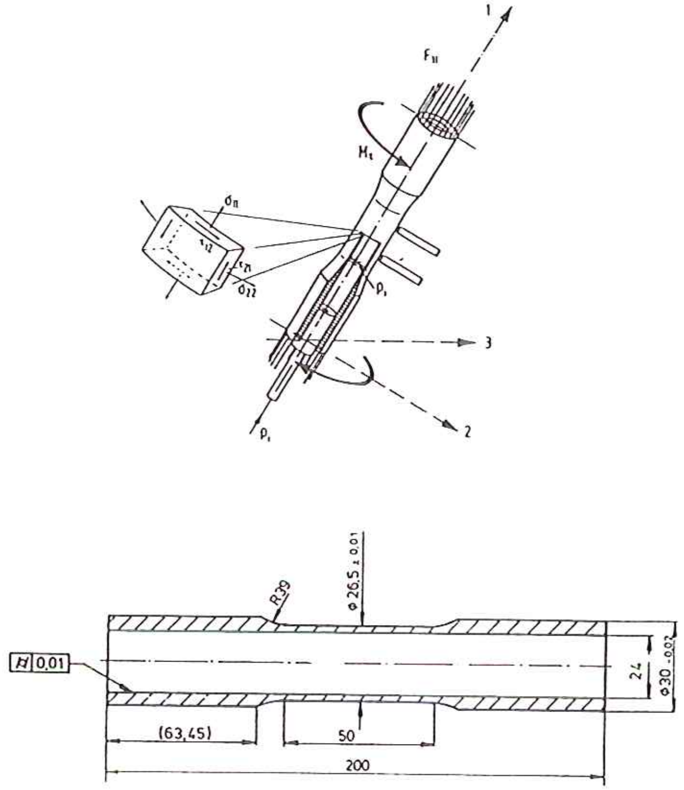

Fig 3 Thin-walled tubular specimen.

axial and shear strain displacement under a defined temperature–time history. The normal test procedure consists of three control loops, that is to say one each for axial and torsional strain and for temperature. Total specimen strain ε_{tot} was calculated by adding thermal ε_{th} and mechanical strains ε_m. A nonlinear function of temperature was used to estimate the thermal coefficient of expansion, $\varepsilon_{th(T)} = A_0 + A_1T + A_2T^2 + A_3T^3$ with $A_0 = -2.261 \times 10^{-2}$, $A_1 = 1.652 \times 10^{-3}$, $A_2 = -1.103 \times 10^{-6}$, $A_3 = 1.235 \times 10^{-9}$.

2.3 *Non-isothermal straining paths*

Initial tests using simple TMF cycles, such as those shown in Table 1 and Fig. 1 with different combined axial and shear strain and temperature cycling, were completed to provide reference data on which to build the predictive methodology. More complex blade cycles with mechanical axial strain or mechanical axial and shear strain defined by analysis were also investigated, Fig. 2.

Table 1. Details of simple thermomechanical strain paths.

Temperature (°C)			Temperature rate (°C s^{-1})		Phase angle (deg)		Strain *versus* temperature	Symbol used Fig. 7
T_1	T_2	T_s	$\dot{\varepsilon} = 10^{-4}$ s^{-1}	$\dot{\varepsilon} = 10^{-5}$ s^{-1}	$\varepsilon - T$	$\gamma - T$		
TMF tensile–compressive strain $\varepsilon_m = 0.6\%, 0.5\%, 0.4\%$ (CCD, CWD $\varepsilon_m = 0.6\%$)								
950 850 750	450 600 550	700 725 650	4.17 2.08 1.67	0.42 0.21 0.17	0, 180 0, 180 0, 180		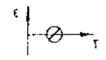	□ 0° ◇ 180°
950 850 450 600	450 600 950 850	450 600 950 850	4.17 2.08 4.17 2.08		−90 −90 90 90		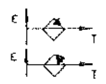	
TMF shear strain $\gamma/\sqrt{3} = 0.6\%$, $\dot{\gamma}/\sqrt{3} = \dot{\varepsilon}$								
950 760	450 450	700 605	4.17 2.58	0.42 0.26		0, 90 0, 90	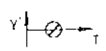	
450 450	950 760	950 760	4.17 2.58	0.42 0.26		90 90	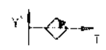	
TMF proportional axial and shear strain $\bar{\varepsilon}_m = 0.6\%$								
950 760 450	450 450 950	700 605 700	4.17 2.58 4.17	0.42 0.26	0 0 −90	0 0 −90	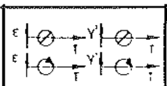	
450 450	950 760	950 760	4.17 2.58	0.42 0.26	90 90	90 90	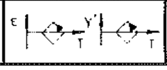	
TMF nonproportional axial and shear strain $\bar{\varepsilon}_m = 0.4\%, 0.5\%, 0.6\%$								
450 600	950 850	700 725	4.17 2.08		180 180	−90 −90	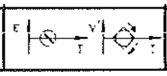	○

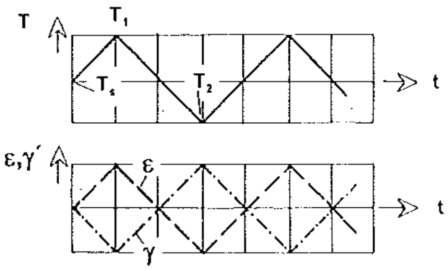

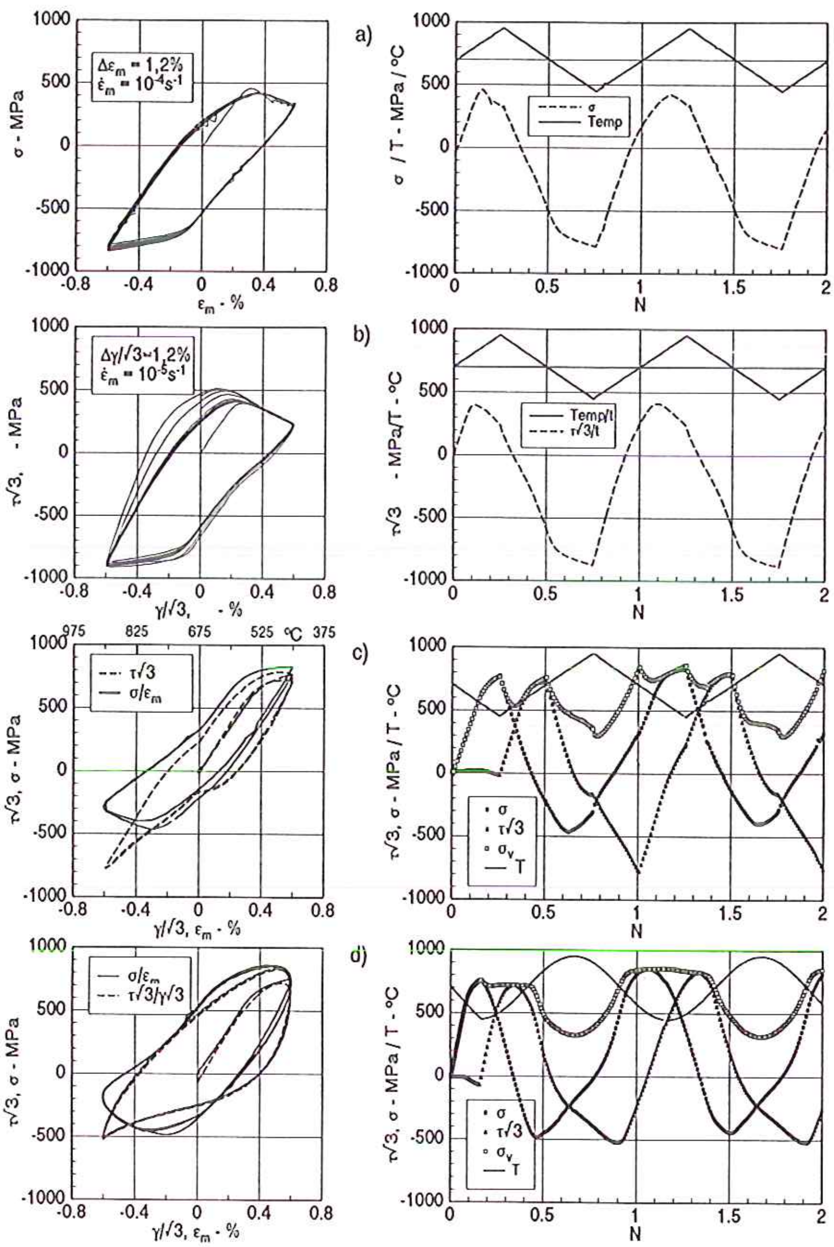

Fig 4 Stress–mechanical strain behaviour and stress response *versus* cycles for simple TMF tests, 450–950°C: (a) linear axial strain ramps, ε–T IP; (b) linear shear strain ramps, $\gamma/\sqrt{3}$–T IP; (c) linear axial and shear strain ramps, ε–T IP, $\gamma/\sqrt{3}$–T CWD; (d) sinusoidal axial and shear strain, ε–T IP, $\gamma/\sqrt{3}$–T OP.

Superimposed creep damage on fatigue life was simulated by holding specimens at maximum temperature for five minutes. In the simple TMF cycles both in-phase and out-of-phase cycles were performed for thermomechancial strain cycling between 450 to 950°C (600 to 850°C, 450 to 760°C). In this simple class sinusoidal nonproportional ε–γ straining paths have been carried out, as described in Table 1. Most of the TMF cyclic tests were conducted for strain ranges of $\bar{\varepsilon} = 0.4$, 0.5 and 0.6 percent at a strain rate of $10^{-4}\ s^{-1}$ and $10^{-5}\ s^{-1}$. The heating and cooling rates were 4.2 K s^{-1} and 0.26 K s^{-1}.

3 Results

3.1 *Simple TMF tests*

In addition to providing reference data for further study, these experiments, were designed to investigate three points. Firstly, strain–temperature phase effects were studied by using in-phase, out-of-phase and diamond TMF cycles, where the axial strain, shear strain or the axial and the shear strain amplitude were held constant, $\varepsilon_m = \bar{\varepsilon} = 0.4$, 0.5 and 0.6%. Does this result in different fatigue lives? Also how do different temperature ranges 450–950°C, 450–760°C and 600–850°C affect fatigue lives? Thirdly, can the isothermal data and the J_2-theory be used to describe the thermomechanical response of IN 738 LC? The results and the answers to these questions will be also used to assess the need of different life prediction techniques.

3.2 *Strain–temperature phase effect, temperature range*

The longest lives were exhibited by those samples which had undergone diamond-type loadings. For these tests, the strain at the maximum temperature was zero. The shortest lives were seen in those tested under sinusoidal nonproportional strain paths. Different temperature mechanical strain phasing, that is linear out-of-phase or in-phase cycling, had a signficant effect on fatigue lives in the temperature range 450°C to 950°C. A crossover of the linear TMF lines with temperature phasing of 0° or 180° is seen at about 10 cycles to failure, Fig. 7(a–e).

Fatigue lives for the different TMF cycles are signficantly less than for an isothermal cycle at the same maximum temperature (6). This suggests that the thermal cycling introduces additional damage associated with thermal inhomogeneities, either microscopically or macroscopically. Some typical cyclic stress–strain curves for the linear TMF cycles are shown in Fig. 4. Linear TMF tests conducted in the temperature range 450°C to 760°C gave longer lives, that is twice more than the tests with the temperature range 450°C to 950°C.

3.3 *Use of isothermal data for predicting nonisothermal behaviour*

Figure 5 shows the hysteresis loops of IN 738 LC subjected to linear in-phase TMF loading under a mechancial strain range of ± 0.6 percent and in a

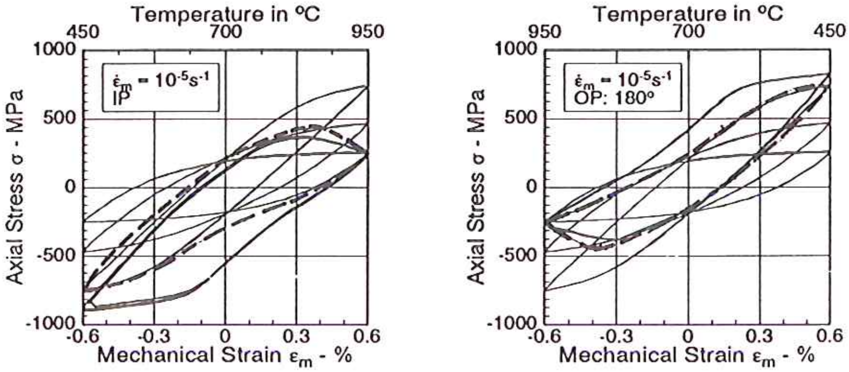

Fig 5 Comparison of TMF and isothermal hysteresis loops.

temperature range 450°C to 950°C, and also the hysteresis loops for other isothermal temperatures under the same conditions. The isothermal loops are used to construct the hypothetical thermomechanical loop (broken line) assuming that the stress response of isothermal loading must be equivalent to nonisothermal loading for definite stress points of the hysteresis loops. Predicted and experimental curves show good correlation at the highest temperature 950°C, although with 450°C the predictions are slightly low. The predicted width of the hysteresis loop, however, is smaller than that observed. The shape of the experimental hysteresis loop tends to be more square.

The above-mentioned behaviour was confirmed by sinusoidal nonproportional straining paths in tension–torsion tests at temperatures between 450 and 950°C with an effective mechanical strain $\bar{\varepsilon} = 0.6$ %, Fig. 6. In this figure the solid line represents the stress loci of TMF tests in the $\sigma\sqrt{3}\tau$ stress space and the broken lines (circles) the stress loci of isothermal tests under the same effective strain but at different temperatures. The experimental stress loci of the TMF and isothermal tests coincide at the highest and lowest temperatures, but discrepancies can be observed at other temperatures. Examination of Fig. 6 indicates, therefore, that J_2-theory is applicable at the highest and lowest temperatures.

3.4 *Fatigue life for complex strain–temperature cycling*

For complex cyclic strain and temperature histories the standard Manson–Coffin damage accumulation law cannot be adequately applied (**3**). Inelastic strain range $\Delta\varepsilon_{min}$ is usually the only material deformation parameter required for measuring damage in the case of purely time-independent deformations. However, functions which include stress, total strain range and inelastic strain range are also proposed to measure the low cycle fatigue damage at elevated

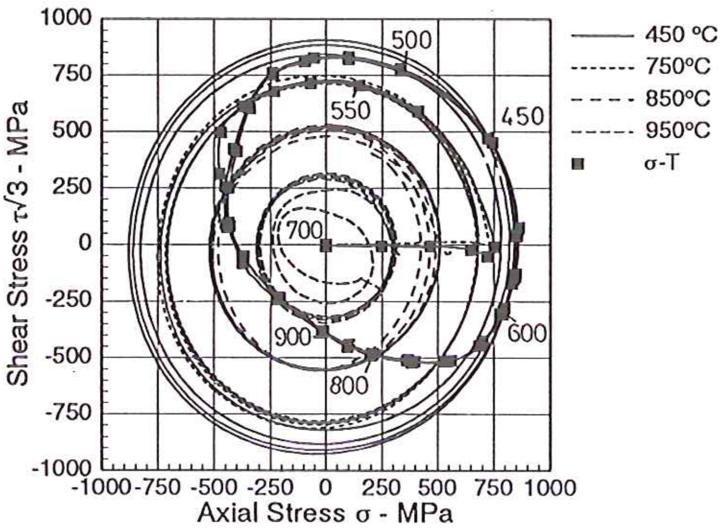

Fig 6 Comparison of TMF and isothermal stress responses for 90° out-of-phase strain cycling, $\bar{\varepsilon} = 0.6\%$, of IN 738 LC.

temperatures (4, 5). Predictions for simple and complex TMF testing conditions are plotted as total mechanical strain range $\Delta\varepsilon_{tot}$, maximum stress range $\Delta\sigma_{max}$, mechanical inelastic strain range $\Delta\varepsilon_{min}$ and energy criteria $\Delta\sigma_{max}\Delta\varepsilon_{tot}$ and $\Delta\sigma_{max}\Delta\varepsilon_{m}$, *versus* cycles to failure in Fig. 7(a–e). The inelastic strain range was taken as the width of the saturated hysteresis loop at zero stress. Although this is not the maximum inelastic strain $\Delta\varepsilon_{min\,max}$, achieved within each cycle, $\Delta\varepsilon_{min}$ was chosen instead of $\Delta\varepsilon_{min\,max}$ because the temperature at which $\Delta\varepsilon_{min\,max}$ was reached was a function of not only the applied strain range and strain temperature cycling. The net tensile or tensile and compressive hysteretic energy ΔW was also used as a measure of fatigue damage, Fig. 7(f). Strain energy is not a linear function in a log–log scale.

It is apparent from Fig. 7(a–e) that significant parameters governing cycles to failure in the TMF tests were the maximum stress range $\Delta\sigma_{max}$, the total strain range $\Delta\varepsilon_{tot}$, the mechanical inelastic strain range $\Delta\varepsilon_{min}$ and the energy expressions $\Delta\sigma_{max}\Delta\varepsilon_{tot}$ and $\Delta\sigma_{max}\Delta\varepsilon_{min}$. It should be noted, however, that the maximum stress range is related to the strain range since increasing the strain range also increases that of the maximum stress. The mechanism of low cycle fatigue failure (damage), (that is in the case of IN 738 LC containing pores and ceramic inclusions only crack extension), suggests that a gradual build-up of damage during a combined strain–temperature cycle is a more realistic mechanism than a sudden, discontinuous crack extension reaching the peak inelastic strain condition. This conclusion may also be deduced from Fig. 8,

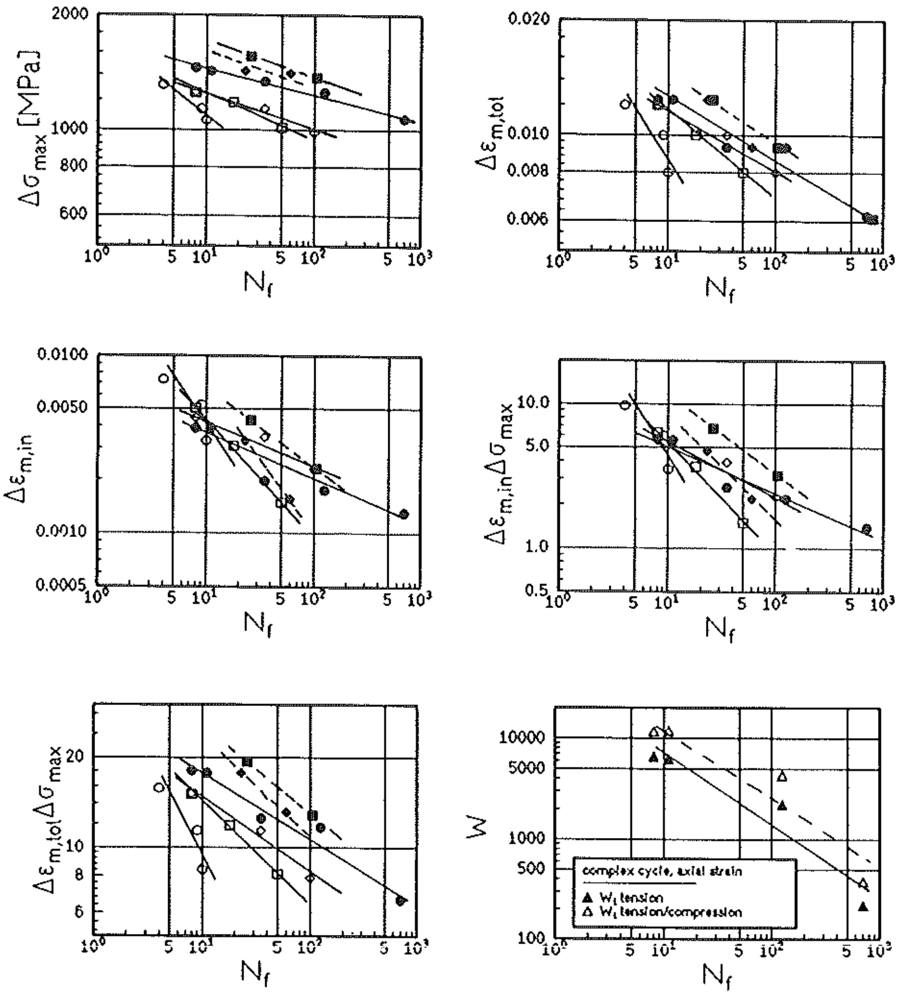

Fig 7 Inelastic strain range, total strain range, maximum stress range and energy criteria *versus* cycles to failure for simple and complex TMF tests of IN 738 LC.

where the stress–mechanical strain response and the possible operative mechanisms are shown.

By using the postulated damage measure $\Delta\sigma_{max}\Delta\varepsilon_{min}$ an empirical failure law like that of Ostergren (4) can be established to predict life for themomechanical cycles.

$$C = \Delta\sigma_{max}\Delta\varepsilon_{min}N_f^{\beta} \qquad (1)$$

where C and β are material constants. Values for C and β:

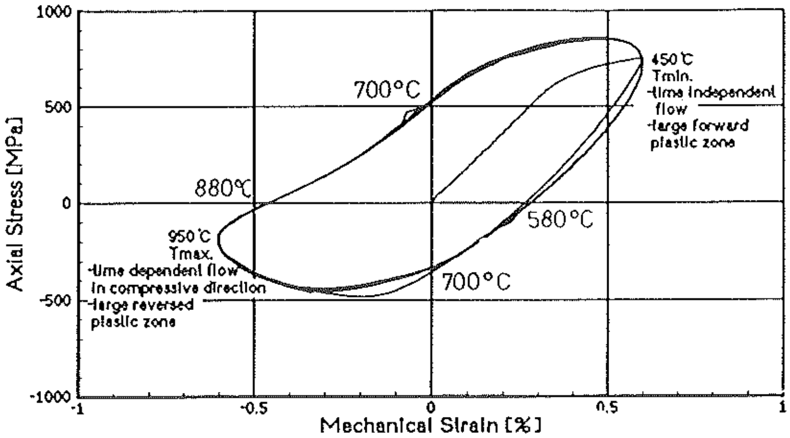

Fig 8 Stress–strain response and the operative mechanisms for a sinusoidal nonproportional TMF test of IN 738 LC, $\bar{\varepsilon} = 0.6\%$, $\dot{\varepsilon} = 10^{-4}\ s^{-1}$, 450–950°C, ε–T = 180°, $\gamma/\sqrt{3}$-T = −90°.

Simple TMF cycles:

linear, axial strain, $\phi(\varepsilon/T) = 0°$ for C = 33.830 MPa m/m, $\beta = 0.789$;

linear, axial strain, $\phi(\varepsilon/T) = 180°$ for C = 12.192 MPa m/m, $\beta = 0.351$;

sinusoidal, $\phi(\varepsilon/T) = 180°$, ε, γ nonproportional for C = 35.087 MPa m/m, $\beta = 0.910$.

Complex TMF cycles:

axial strain for C = 10.600 MPa m/m, $\beta = 0.323$;

axial and torsional strain for C = 39.108 MPa m/m, $\beta = 0.539$;

axial and torsional strain, 5 min hold time, for C = 57.620, MPa m/m, $\beta = 0.789$.

The range of the ratio $N_{f\,sim}/N_{f\,exp}$ is 0.7–1.2 (2.0).

The results of IN 738 LC can be correlated without a frequency term. This fact suggests that, in this alloy, the time dependency of damage may be described through the variation of $\Delta\varepsilon_{in}$ is not time dependent, which agrees with (4).

4 Discussion and Summary

This study aimed to predict TMF behaviour using isothermal data at the maximum and minimum temperatures of a TMF-linear cycle; the correlation between predicted and observed behaviour was usually good, especially at the higher temperatures. However, it was also shown that the isothermal data cannot completely predict the TMF response. The agreement between isothermal and TMF data can be attributed to two facts. Firstly, the saturated TMF-responses at minimum and maximum temperatures are the same as in the isothermal cases. For IN 738 LC test data indicates saturation within the first three cycles both in isothermal and TMF cases. In addition it does not appear to be

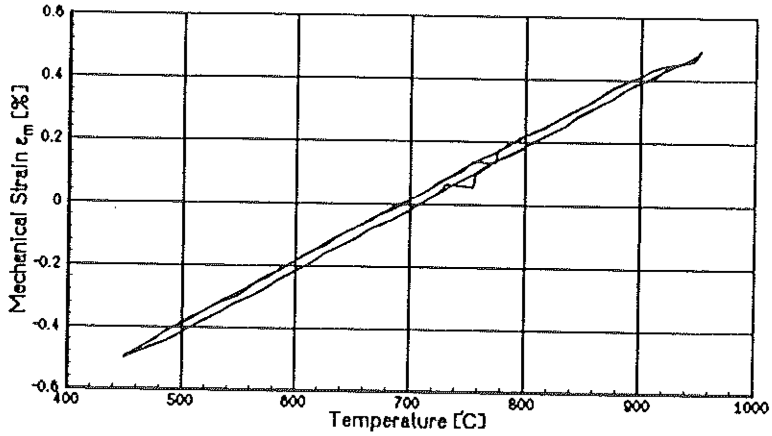

Fig 9 Mechanical strain *versus* temperature for a linear TMF-test, 450–950°C.

dependent on cyclic hardening or temperature history (6). The hardening/softening behaviour shown in isothermal cyclic loading is also seen in thermomechanical cycling although the material parameters depend on temperature. Linear interpolation of the parameters between these temperatures led to inconsistent isothermal and non-isothermal predictions.

Secondly, the TMF behaviour can be predicted by the isothermal parameters, where the strain range and peak temperature levels during TMF-cycling activate the same mode of inelastic deformation as in isothermal cycling. For IN 738 LC this seems to be the case (6).

Another class of metals exhibits cyclic hardening dependent on temperature history. Representatives of this class of metals are 304 and 316 stainless steels (7), Hastelloy X (8) and 1070 steel (9).

In thermomechanical cycling, the strain temperature phasing can have an important influence on life. Results from IN 738 LC tests using simple linear TMF cycles indicate a possible shift in life of up to a factor of 10, Fig. 7(a-e). The lines also cross due to different temperature phasing. An investigation into whether or not the J_2-theory may be used to describe the thermomechanical response of IN 738 LC is outlined in this paper. The study indicates that the classical plasticity theory is a convenient and useful method for peak temperature work.

The fatigue lives of IN 738 LC are compared on the basis of the mechanical inelastic strain range $\Delta\varepsilon_{min}$, maximum stress range $\Delta\sigma_{max}$, total strain range $\Delta\varepsilon_{tot}$ and energy criteria, Fig. 7(f). However, correlations based on these criteria do not allow development of a common theory for the TMF data. They may, on the other hand, be classified.

In the analysis of the inelastic strain method, both test data and Fig. 9, clearly reveal that in many cases the elastic portion of the mechanical strain $\Delta\varepsilon_{mel}$ is either greater than or equal to the inelastic strain range $\Delta\varepsilon_{min}$. The contribution of the elastic strain component to the damage cannot be neglected. To predict life on such a basis, it is first necessary to determine the inelastic and elastic lines, and the strain range partitioning inelastic strain range *versus* life relations, experimentally. Many assumptions have to be made for such an analysis.

The present investigations on IN 738 LC showed better correlation with energy approaches on $\Delta\varepsilon_{min}$ or $\Delta\varepsilon_{tot}$ and $\Delta\sigma_{max}$.

The damage of IN 738 LC is effectively only of crack propagation. Even in normal fatigue crack propagation analysis, the crack closure effect has been recognized and the effective stress intensity has been used to describe the crack growth rate. The influence of mean stress must also be taken into account. The quantity $\Delta\sigma_{max}\Delta\varepsilon_{min}$ or $\Delta\sigma_{max}\Delta\varepsilon_{tot}$ is therefore a direct measure of damage and has the advantage of incorporating stress (involved in propagating the crack) and strain parameters.

Complex TMF cycle tests representing strain temperature time profiles in critical regions of a blade gave longer lives when compared with simple linear TMF tests. Since this high-temperature deformation occurs at larger compressive strains, a shift in mean stress is seen in all tests. The approach used to describe fatigue with linear TMF cycles can therefore be expected to be conservative. A five-minute hold at the maximum temperature, Fig. 2, results in shorter lives at high inelastic strains than those resulting from more complex cycles but without hold time. A few complex TMF tests have included axial and torsional strain time temperature phasing, Fig. 2. These tests results did not show longer lives than those from simple axial strain time temperature phasing tests at the same mechanical effective strain $\bar{\varepsilon}$. However, there are different main crack propagation directions for the different complex cycles. Without a torsional strain amplitude, the macroscopic crack direction is perpendicular to the tube axis; in axial and torsional TMF tests, crack directions are inclined by 30° to 45° to the axis of the specimens. Since the saturated state of IN 738 LC is independent of thermomechanical straining path, the maximum saturation stress range and the limiting values produced by hardening/softening should also be independent of the thermomechanical straining path, and can therefore be evaluated using experimental data obtained from simple or linear straining paths. It is thus reasonable to conclude that in this case, simple TMF data are sufficient to evaluate some complex TMF cycles.

The objective of TMF tests is also to develop a fatigue life prediction method. Key elements of this method are: component analysis, TMF testing and analytical evaluation of material behaviour.

Acknowledgements

The study presented here is part of an extensive investigation into IN 738 LC alloy under multiaxial states of stress and temperature history. The financial support for this research, provided by Deutsche Forschungsgemeinschaft (DFG), is gratefully acknowledged.

References

(1) EMBLEY, G. T., RUSSEL, E. S. (1984) Thermal–mechanical fatigue of gas turbine bucket alloys, in *Proceedings, First Parsons International Turbine Conference*, Inst. Mechanical Engineers, London, pp. 157–164.

(2) COOK, T. S., KIM, K. S., McKNIGHT, R. L. (1988) Thermal mechanical fatigue of cast Rene 80, *Low Cycle Fatigue*, ASTM, STP, (Eds. H. D. Solomon *et al.*), pp. 692–768.

(3) COFFIN, L. F. (1953) A study of the effects of cyclic thermal stresses on a ductile metal, paper 53-A76, American Society for Mechanical Engineers, New York.

(4) OSTERGREN, W. J. (1976) A damage function and associated failure equations for predicting hold time and frequency effects in elevated temperature low cycle fatigue, *JTEVA*, 4, pp. 327–339.

(5) HOLFORD, G. R., SALTSMAN, J. F. (1987) Calculation of thermo-mechancial fatigue life based on isothermal behaviour, in *Proc. Thermal Stress Material Deformation and Thermomechanical Fatigue*, ASME, PVP, pp. 9–21.

(6) ZIEBS, J., MEERSMANN, J., KUHN, H. J. (1992) High temperature inelastic deformation of IN 738 LC under uniaxial and multi-axial loading, *Low Cycle Fatigue and Elastic-Plastic Behaviour of Materials - 3*, (Ed. K. T. Rie), Elsevier Applied Science, London, pp. 248–255.

(7) OHNO, N. (1990) Recent topics in constitutive modelling of cyclic plasticity and viscoplasticity, *Appl. Mech. Rev.*, **43**, pp. 283–295.

(8) ROBINSON, D. N., BARTOLOTTA, P. A. (1985) Viscoplastic constitutive relationships with dependence on thermo-mechanical history, NASA CR-174836.

(9) SEHITOGLU, H., KASARET, M. (1986) Observations of material behaviour under isothermal and thermo-mechanical loading, *J. Eng. Mat. Tech.* **108**, pp. 192–198.